A Circuit Model of Probes in Dual-Mode Cavities

KAWTHAR A. ZAKI, SENIOR MEMBER, IEEE, CHUNMING CHEN, STUDENT MEMBER, IEEE, AND ALI E. ATIA, FELLOW, IEEE

Abstract—**An accurate model of coaxial probes used as input and output ports in dual-mode cavities (either air-filled or dielectric-loaded) is presented. The model precisely predicts such empirically observed phenomena as limited out-of-band isolation, generation of extra transmission zeros, and asymmetric responses. The model parameters can be determined from simple measured data. It is shown how the model can be used in the analysis and synthesis of canonical dual-mode filters. Experimental verification of the model for several configurations showed excellent agreement with theory.**

I. Introduction

CANONICAL dual-mode filters realized in empty waveguide resonators [1] or in dielectric-loaded resonators [2], [3] require that the input and output ports of the filters be located in the same physical cavity. The simplest port configuration employs two coaxial connectors, with their center conductors extending into the resonators at 90° to each other, as shown in Fig. 1. The coaxial probes in Fig. 1 couple to the radial electric fields of each of the two orthogonal dual modes of the resonator. Although this coupling configuration is simple, it has been observed experimentally that the maximum isolation achievable between the input and output ports is limited (to about 30 dB) [1]. In [3], it was also observed experimentally in a four-pole filter that if the coupling screw in the input/output cavity is in orientation A of Fig. 1, a pair of extra transmission zeros are created in the filter's response. Orientation B, on the other hand, does not introduce these real transmission zeros. This behavior is attributed to spurious coupling between the input and output probes.

The objective of the present paper is to develop a circuit model that predicts the precise behavior of two probes in a dual-mode cavity. The circuit model could be used in the analysis and calculation of the frequency of any given filter structure. The model's properties could also be included in any synthesis procedure in which this type of coupling is used. Experimental verification of the model is carried out and the measurements also provide useful data for the design and prediction of canonical dual-mode filters responses.

Manuscript received April 19, 1988; revised August 1, 1988. This work was supported by the National Science Foundation under Grant ECS-8617534.

K. A. Zaki and C. Chen are with the Department of Electrical Engineering, University of Maryland, College Park, MD 20742.

A. E. Atia is with the COMSAT Corporation, Clarksburg, MD 20871.

IEEE Log Number 8823768.

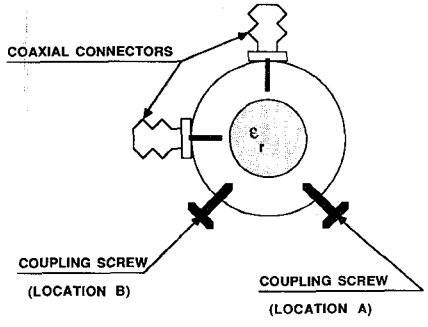

Fig. 1. Cross section of dual-mode cavity with input and output coaxial probes.

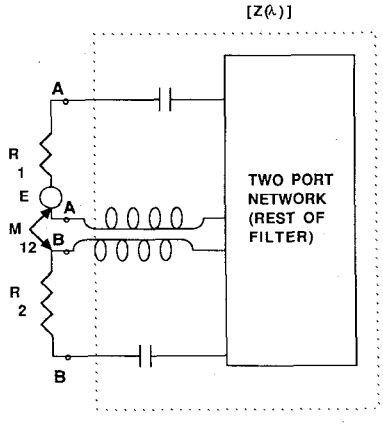

Fig. 2. Circuit model of the probes neglecting coupling by higher order modes.

II. Circuit Model

The equivalent circuit model usually employed of two probes coupled to a dual-mode cavity in a multiple coupled cavity filter is shown in Fig. 2. The external Q's are represented by the resitances R_1 and R_2; the series LC circuits represent the two dual modes of resonance in the cavity, and the two-port network represents the rest of the filter. The coupling M_{12} between the two resonant dual modes is produced by means of a coupling screw oriented at a 45° angle with respect to each probe's direction. This model does not properly predict the observed measured frequency responses of canonical dual-mode filters, such as the limited out-of-band isolation [1] and the presence of two extra transmission zeros in the filter's responses for certain orientations of the coupling rows [3]. The observed limited out-of-band isolation can be interpreted as being

0018-9480/88/1200-1740$01.00

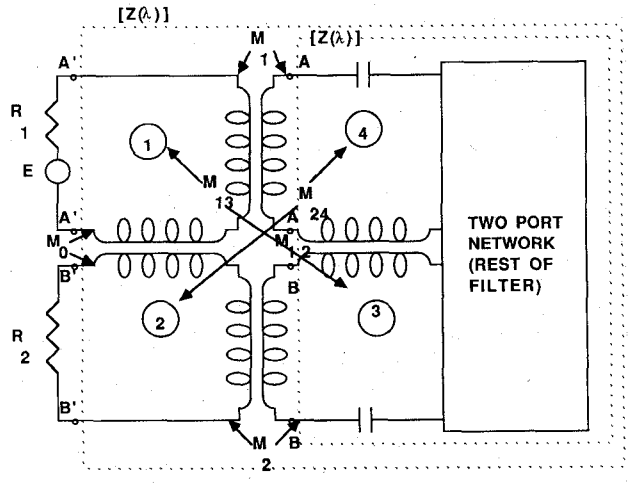

Fig. 3. Circuit model of the probes including the effect of coupling by higher order modes.

due to an additional nonresonant (other than M_{12}) coupling mechanism. This coupling exists because of the effects off evanescent and higher order mode fields of the resonator. The effects of these fields in the frequency range of interest are normally modeled by constant reactances [4]. The model shown in Fig. 3 is one possible form that accounts for the additional nonresonant coupling effects. This model represents each probe by a coupling loop. In addition, to the resistances R_1 and R_2 representing the external Q's of the probes, the coupling loops (shown by the circled numbers 1 and 2 in Fig. 3) contain the couplings M_1, M_2, M_0, M_{13}, and M_{24}. The inclusion of these couplings properly models the observed frequency response of the filters, as will be shown subsequently. Each of the shown couplings has a physical interpretation through the fields existing within the resonators. Consider the field distributions of the resonator shown in Fig 4. The theoretical (unperturbed) dielectric resonator fields of Fig 4(a) for the lowest degenerate, orthogonal hybrid (HEH_{11}) modes are obtained by the methods of [5] and [6]. The presence of the probes disturbs these fields, and to satisfy the boundary conditions of vanishing tangential electric field on the probes, the fields become nonorthogonal, as shown in Fig. 4(b). Due to the finite thickness of the probes, the perturbed electric field components of mode 1 perpendicular to probe 2 induce circumferential currents in this probe. These currents result in inductive coupling between the probes modeled by M_0. The larger the thickness (diameter) of the probe, the larger this coupling becomes. These same components of mode 1 perturbed electric fields induce currents in the circumference of the coupling screw, resulting in coupling to the resonator's field, indicated by M_{13}. A similar interpretation of the coupling M_{24} can be made. Couplings M_1 and M_2 represent the change in the levels of characteristic impedance between the coaxial probes and the waveguide dielectric-loaded resonator. An equivalent circuit model similar to that shown in Fig. 3 was presented by Bell [7] for the representation of canonical asymmetric filters.

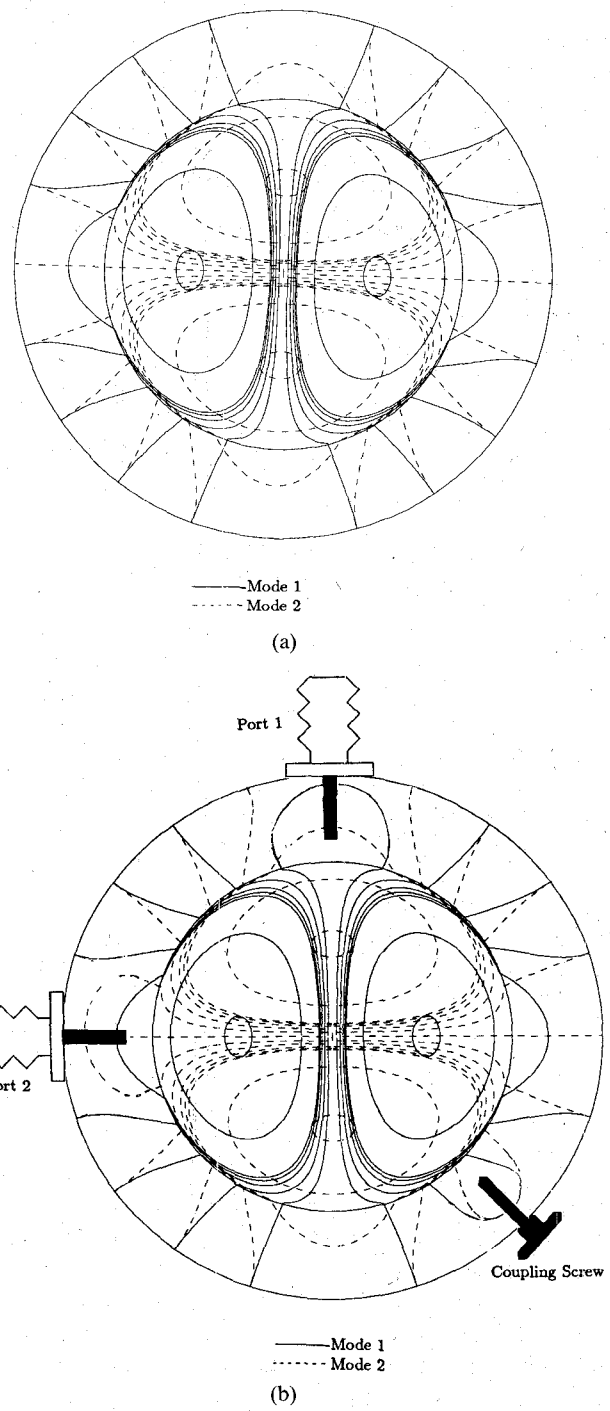

Fig. 4. (a) Theoretical (unpertubed) electric field distribution of HEH_{11} mode in a dielectric loaded resonator. (b) Perturbed electric field distribution of the modes due to the probe and coupling screw.

The synthesis of coupled resonator filters when the probe model is included can follow the procedure given in [7]. Alternatively, simple modifications to the procedures of [8] can be made to accommodate the probe's model, as follows.

Let the two-port open circuit impedance matrices of the multiple coupled cavity filter's models shown in Fig. 2 and Fig. 3 at reference planes $(A \cdot A, B \cdot B)$ and $(A' \cdot A', B' \cdot B')$ be $[Z(\lambda)]$ and $[Z'(\lambda)]$, respectively. Determination of element values of the coupling matrix which realizes $[Z(\lambda)]$

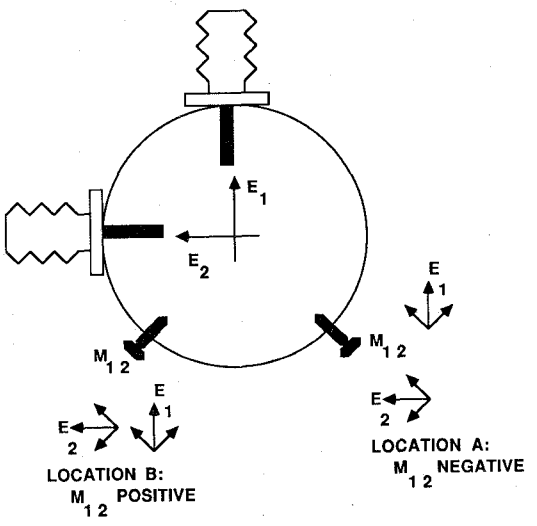

Fig. 5. Electric field components parallel and perdicular to the coupling screws for locations A and B.

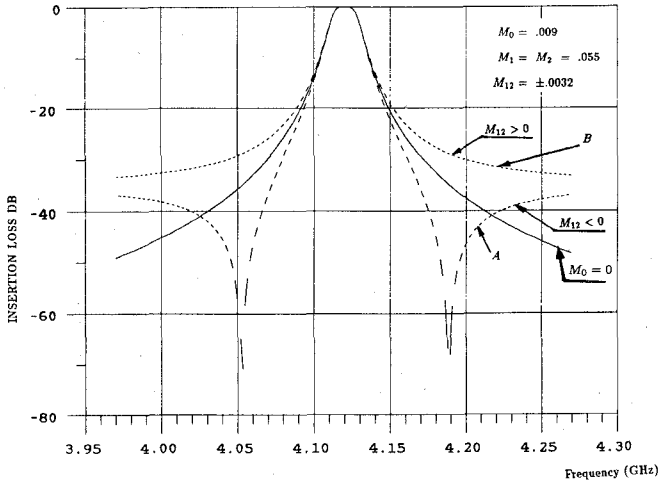

Fig. 6. Computed insertion loss response of two-pole filters.

with a given coupling topology from a given transfer function can be carried out using the procedures in [8]. To use the same procedures it is only necessary to relate $[Z(\lambda)]$ to $[Z'(\lambda)]$ and the probe's parameters (M_0, M_1, M_2, M_{13} and M_{24}) shown in Fig. 3. Simple analysis using loop equations can be carried out on the model of Fig. 3 to show that this relationship is

$$[Z'(\lambda)] = -jM_0\begin{bmatrix}0 & 1\\ 1 & 0\end{bmatrix} - \begin{bmatrix}M_1 & M_{13}\\ M_{24} & M_2\end{bmatrix}[Z(\lambda)]^{1}\begin{bmatrix}M_1 & M_{24}\\ M_{13} & M_2\end{bmatrix}. \quad (1)$$

In order to achieve the objective of modeling the coupling probes of the two-port network representing the rest of the filter in Fig. 3 may be replaced by short circuits; the resulting model consists of a two-pole filter. The transfer function $t(\lambda)$ (defined by $|t(\lambda)|^2 =$ output power in R_2/available power from E) of such a filter is readily calculated in terms of the element values of the model to

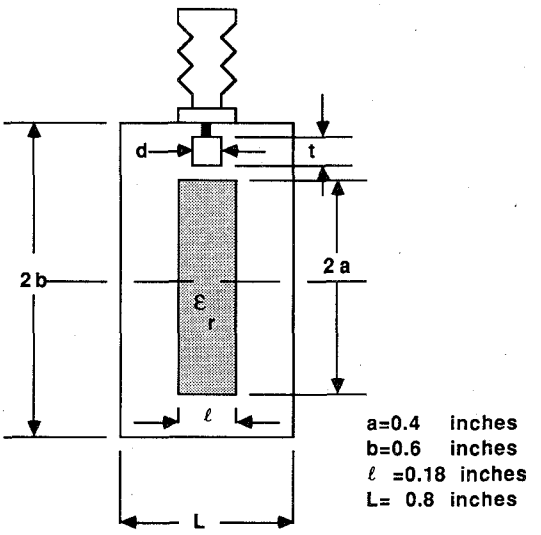

Fig. 7. Configuration of experimental resonator and probe.

be

$$t(\lambda) = -2j\sqrt{R_1R_2}\,\frac{b_0 + b_1\lambda + b_2\lambda^2}{a_0 + a_1\lambda + a_2\lambda^2} \quad (2)$$

where

$$\lambda = \left(\frac{\omega}{\omega_0} - \frac{\omega_0}{\omega}\right)$$

is the normalized low-pass frequency variable and

$$a_0 = R_1R_2M_{12}^2 - M_0b_0 - M_{13}M_{24}C_0 - M_1M_2C_1 + j2M_{12}C_2$$
$$a_1 = -2M_0b_1 + j\{R_1(M_2^2 + M_{24}^2) + R_2(M_1^2 + M_{13}^2)\}$$
$$a_2 = -(R_1R_2 + M_0^2)$$
$$b_0 = M_{12}(M_1M_2 - M_0M_{12} + M_{13}M_{24})$$
$$b_1 = M_1M_{24} + M_2M_{13}$$
$$b_2 = M_0$$
$$C_0 = M_0M_{12} - M_{13}M_{24} + M_1M_2$$
$$C_1 = M_0M_{12} - M_{13}M_{24} - M_1M_2$$
$$C_2 = R_1M_2M_{24} + R_2M_1M_{13}.$$

Several properties of this transfer function are observed. As $\lambda \to \infty$, $t(\lambda) \to 2jM_0\sqrt{R_1R_2}/M_0^2 + R_1R_2$. Assuming that the spurious coupling $|M_0| \ll \sqrt{R_1R_2}$, the input/output isolation of this filter is limited to approximately $-20\log|2M_0/\sqrt{R_1R_2}|$ dB. It can be easily shown from (1) and the properties of $[Z(\lambda)]$ that for filters of order $n \geq 2$, this same value of isolation is achieved. Further, the transfer function of (2) has zeros of transmission λ_{Z_1}, λ_{Z_2} at

$$\lambda_{Z_{1,2}} = \frac{-b_1 \pm \sqrt{b_1^2 - 4M_0b_0}}{2M_0}. \quad (3)$$

The transmission zeros are real if $b_1^2 - 4M_0b_0 \geq 0$, and are complex if $b_1^2 - 4M_0b_0 < 0$. For the most commonly used parameters, it can be shown that $\lambda_Z^2 \simeq -M_1M_2M_{12}/M_0$. Since (M_1M_2/M_0) is always positive in this configuration,

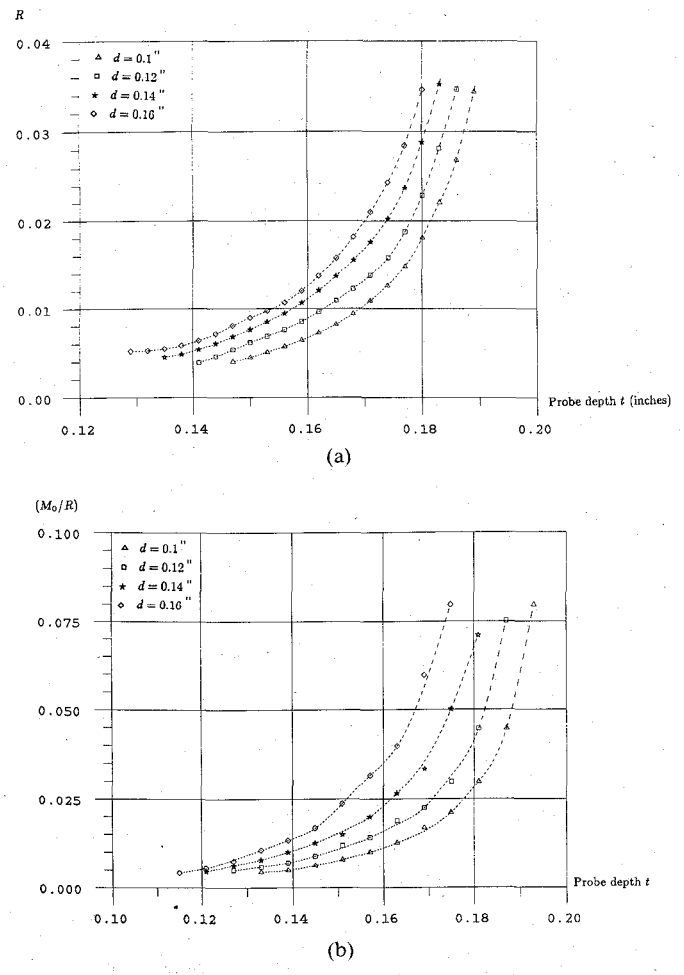

Fig. 8. (a) Variation of R with probe depth and thickness. (b) Variation of (M_0/R) with probe depth and thickness.

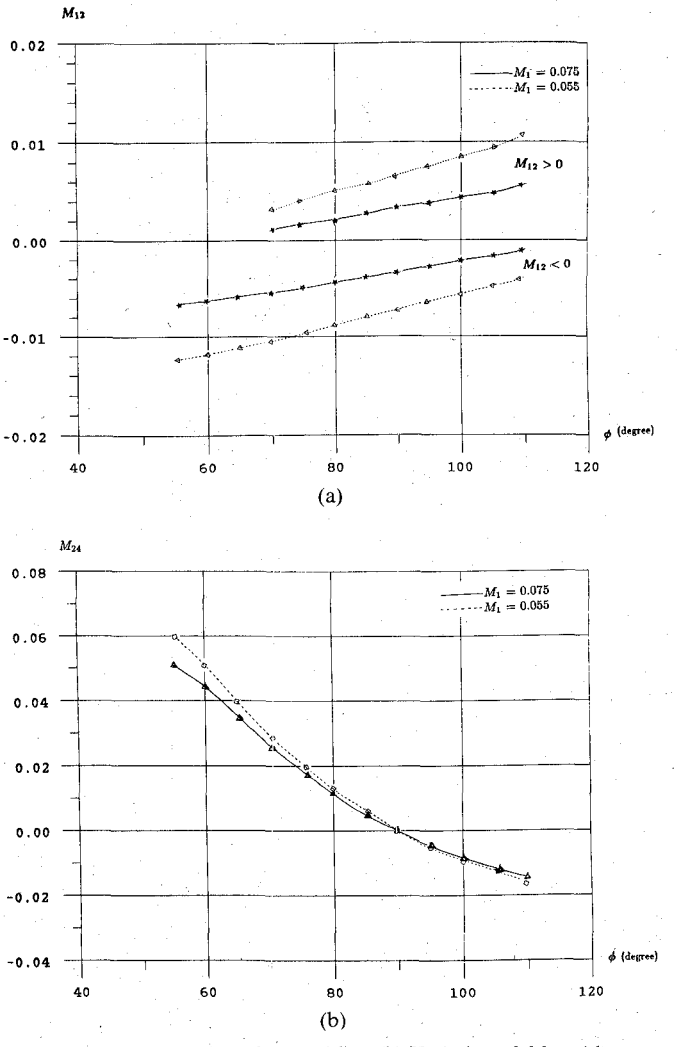

Fig. 9. (a) Variation of M_{12} with ϕ. (b) Variation of M_{24} with ϕ.

it is seen that λ_Z^2 will be positive if M_{12} is negative and vice versa. The coupling M_{12} is negative for the coupling screw location A and positive for location B shown in Fig. 1. This can be seen from the relative directions of the elctric field components of the fields E_1 and E_2, parallel and perpendicular to the coupling screws, as shown in Fig. 5. When the components of E_1 and E_2 are both in the same direction as the coupling screw, M_{12} is negative, and when these components are in opposite direction, the coupling M_{12} is positive, since these components must satisfy the boundary condition of vanishing total tangential electric field on the perfectly conducting screw. This therefore explains the experimentally observed phenomena of an extra pair of transmission zeros present in the response of four-pole canonical dual-mode filters having input and output coaxial probes in the same cavity [3]. Fig. 6 shows the computed response of three two-pole filters having identical external Q's (R_1, R_2) and M_{12}. The solid curve in this figure corresponds to the case where $M_0 = 0$; i.e., the input/output probes are in two different cavities. The two dotted curves A and B in Fig. 6 correspond to locations A and B of the coupling screw of Fig. 1, respectively. The effect of the sign of M_{12} on the response is clearly evident in the presence of the two transmission zeros in curve A.

III. Experimental and Computed Results

Parameters of the equivalent circuit can be determined from the above equations using measured values of $|t(\infty)|$, λ_{Z_1}, and λ_{Z_2}. The values of R_1, R_2, and M_{12} are determined from the one-port phase measurements described in [9].

Experimental measurements were performed to determine the variation of the various couplings with the angle ϕ between the two probes. From a large number of measurements it was found that the coupling M_0 is almost independent of all the parameters of the coupling structure, except the probe's depth and diameter. Thicker and deeper probes produce larger M_0. Fig. 7 shows the configuration of the experimental probe and resonator. Variations of the input resistance R (reciprocal of the external Q) and the coupling M_0 (normalized to R) with the probe depth for various probe thicknesses are shown in Fig. 8(a) and (b), respectively. Typical measured data showing the variation of the couplings M_{12} and M_{24} with the angle ϕ between the probes are shown in Fig. 9(a) and (b).

When used as a two-pole filter, the filter response is highly dependent on the angle ϕ. The model of Fig. 3 accurately predicts these responses, including the locations of the transmission zeros, the asymmetry of the response,

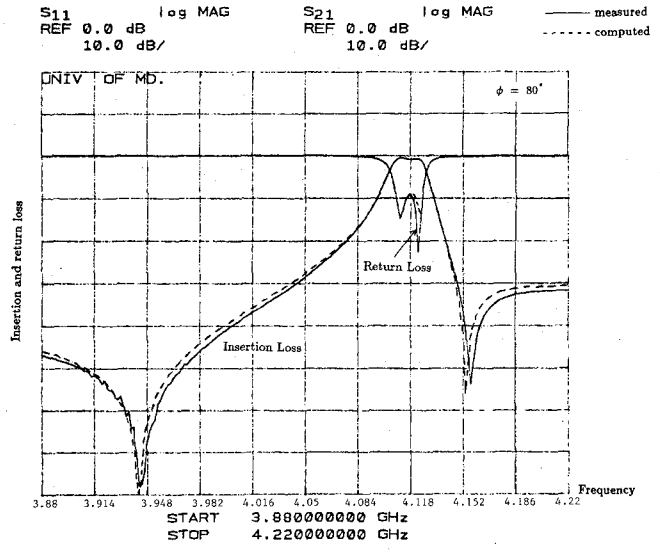

(a)

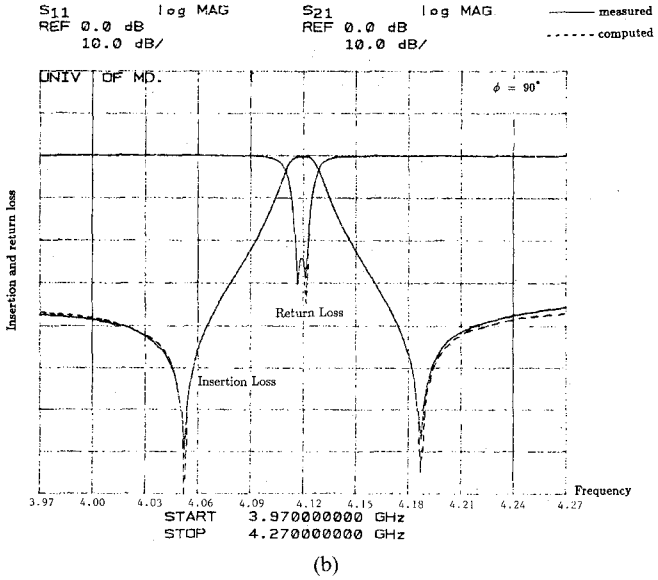

(b)

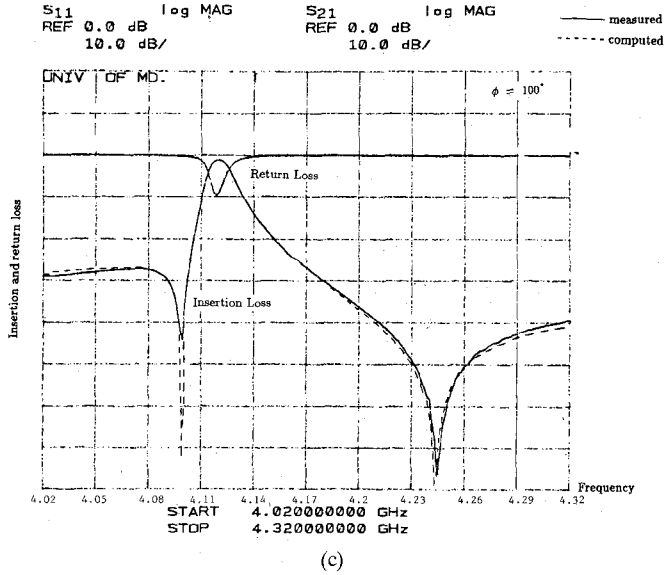

(c)

Fig. 10. (a) Insertion and return loss versus frequency. (b) Insertion and return loss versus frequency. (c) Insertion and return loss versus frequency.

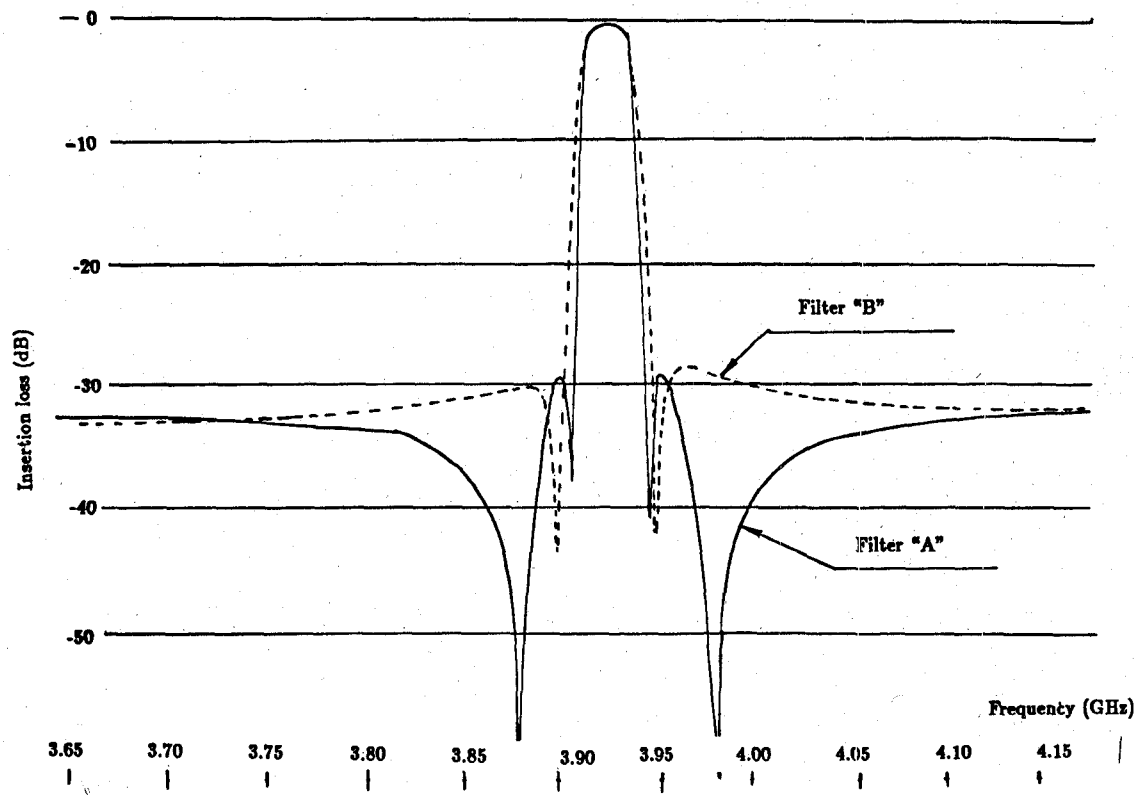

Fig. 11. Measured wide-band insertion loss responses of two four-pole canonical dual-mode filters.

and the maximum achievable out-of-band isolation. Typical measured and computed data depicting the accuracy of the model are given in Fig. 10. Finally, Fig. 11 shows the response of two four-pole filters with positions of coupling screws A and B as shown in Fig. 1, indicating the presence of the two extra transmission zeros due to the presence of the coupling M_0.

IV. Conclusion

The circuit model presented of two coaxial probes in a dual-mode cavity accurately predicts all the behavior of the circuits using this type of configuration. Extensive measurements were carried out and the corresponding responses of the models were computed and compared. There is very limited control on how small the spurious coupling M_0 can be made. Although in higher order filters the minimum value of the out-of-band isolation can be slightly improved, there is always a limit on the maximum achievable isolation which is set by the presence of the spurious coupling M_0.

References

[1] A. E. Williams and A. E. Atia, "Dual-mode canonical waveguide filters," *IEEE Trans. Microwave Theory Tech.*, vol. MTT-25, pp. 1021–1025, Dec. 1977.

[2] S. J. Fiedzinsko, "Dual-mode dielectric resonator loaded cavity filters," *IEEE Trans. Microwave Theory Tech.*, vol. MTT-30, pp. 1311–1316, Sept. 1982.

[3] K. A. Zaki, C. Chen, and A. E. Atia, "Canonical and longitudinal dual-mode dielectric resonator filters without iris," *IEEE Trans. Microwave Theory Tech.*, vol. MTT-35, pp. 1130–1135, Dec. 1987.

[4] C. G. Montgomery, R. H. Dicke, and E. M. Purcell, Ed., *Principles of Microwave Circuits* (vol. 8, Radiation Laboratory Series). New York: McGraw-Hill, 1948, ch. 7.

[5] K. A. Zaki, and C. Chen, "Intensity and field distribution of hybrid mode in dielectric loaded waveguides," *IEEE Trans. Microwave Theory Tech.*, vol. MTT-33, pp. 1442–1447, Dec. 1985.

[6] K. A. Zaki and C. Chen, "New results in dielectric loaded resonators," *IEEE Trans. Microwave Theory Tech.*, vol. MTT-34, pp. 815–824, July 1986.

[7] H. Clark Bell, Jr., "Canonical asymmetric coupled-resonator filters," *IEEE Trans. Microwave Theory Tech.*, vol. MTT-30, pp. 1335–1340, Sept. 1982.

[8] A. E. Atia, A. E. Williams, and R. W. Newcomb, "Narrow-band multiple-coupled cavity synthesis," *IEEE Trans. Circuits Syst.*, vol. CAS-21, pp. 649–655, Sept. 1976.

[9] A. E. Atia and A. E. Williams, "Measurement of inter-cavity coupling," *IEEE Trans. Microwave Theory Tech.*, vol. MTT-23, pp. 519–522, Aug. 1975.

Kawthar A. Zaki (SM'85) received the B.S. degree (with honors) from Ain Shams University, Cairo, Egypt, in 1962 and the M.S. and Ph.D. degrees from the University of California, Berkeley, in 1966 and 1969, respectively, all in electrical engineering.

From 1962 to 1964, she was a Lecturer in the Department of Electrical Engineering, Ain Shams University. From 1965 to 1969, she held the position of Research Assistant in the Electronic Research Laboratory, University of California,

Berkeley. She joined the Electrical Engineering Department, University of Maryland, College Park, in 1970, where she is presently Professor of Electrical Engineering. Her research interests are in the areas of electromagnetics, microwave circuits, optimization, computer-aided design, and optically controlled microwave and millimeter-wave devices.

Dr. Zaki is a member of Tau Beta Pi.

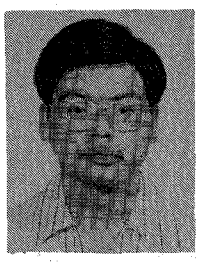

Chunming Chen (S'85) was born in Taiwan, Republic of China, in 1958. He received the B.S. degree from the National Tsing Hua University, Taiwan, in 1981 and the M.S. degree from the University of Maryland, College Park, in 1985, both in electrical engineering. Since 1984, he has worked as a research assistant in Department of Electrical Engineering, University of Maryland, College Park. He is now working towards the Ph.D. degree in the area of microwave components and circuits.

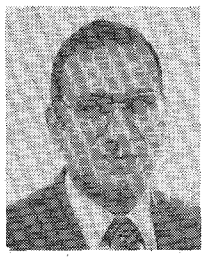

Ali E. Atia (S'67–M'69–SM'78–F'87) received the B.S.E.E. degree from Ain Shams University, Cairo, Egypt, and the M.S.E.E. and Ph.D. degrees from the University of California at Berkeley.

Prior to joining COMSAT in 1969, he held various research and teaching positions at both these universities. As a Senior Scientist in the Microwave Laboratory at COMSAT Laboratories, Dr. Atia has made original contributions to satellite transponder and antenna technologies, most notably the development of the dual-mode microwave filters technology. He has also made significant contributions to several satellite programs, including INTELSAT IV-A, V, V-A, VI, ARABSAT, AND AUSSAT. He was responsible for the design, implementation, qualification, and testing of major subsystems in COMSAT's NASA ATS-F propagation experiment and the COMSTAR *Ka*-band beacon experiment. Presently he is Senior Director of Communications Engineering in COMSAT Systems Division, Clarksburg, MD, responsible for all communications systems design, integration, implementation, and testing under contracts with various government and commercial customers.

Dr. Atia is an Associate Fellow of the AIAA and a Member of Sigma Xi.